Polymer 51 (2010) 84–91

Contents lists available at ScienceDirect

Polymer

journal homepage: www.elsevier.com/locate/polymer

The effect of sulfonic acid groups within a polyhedral oligomeric silsesquioxane containing cross-linked proton exchange membrane

Ying-Chieh Yen [a], Yun-Sheng Ye [a], Chih-Chia Cheng [a], Chu-Hua Lu [a], Li-Duan Tsai [b], Jieh-Ming Huang [c], Feng-Chih Chang [a,*]

[a] Institute of Applied Chemistry, National Chiao Tung University, Hsinchu, Taiwan
[b] Material and Chemical Research Laboratories, Industrial Technology Research Institute, Chutung, Taiwan
[c] Department of Chemical and Materials Engineering, Van Nung Institute of Technology, Chungli, Taiwan

ARTICLE INFO

Article history:
Received 5 August 2009
Received in revised form
16 October 2009
Accepted 16 November 2009
Available online 26 November 2009

Keywords:
POSS
PEM
SPEEK

ABSTRACT

In this study, polyhedral oligomeric silsesquioxane (POSS) moieties were incorporated into sulfonated poly(ether ether ketone) (SPEEK) to form a new cross-linked proton exchange membrane (PEM). The distribution of the POSS containing cross-linkers with or without sulfonic acid groups dictates the water behavior and connectivity of hydrophilic domains of the PEM. A PEM formed by incorporating 17.5 wt% of the cross-linker (containing POSS macromer and sulfonic acid groups) into SPEEK exhibits high proton conductivity (0.0153 S/cm), low methanol permeability (1.34×10^{-7} cm^2/s), and high selectivity (1.14×10^5 Ss/cm^3).

1. Introduction

Proton exchange membranes (PEMs) providing ionic pathways for proton transfer are key component of the direct methanol fuel cell (DMFC). Nafion, one of the most studied material for application as PEM, exhibits both chemical and physical stabilities at moderate temperature and high proton conductivity through its highly interconnected hydrophilic channels [1]. Sulfonated polymers, such as sulfonated poly(ether sulfone) (SPES), poly(benzimidazole) (SPBI), poly(ether ether ketone) (SPEEK), and polyimide (SPI), are also potential candidates for use in PEMs [2–13] but these drawbacks including cost, durability, methanol crossover, and etc limit their applications [1–13]. To overcome these drawbacks, numerous new or modified materials possessing reinforced sulfonated polymers were proposed [14–21]. Cross-linked PEMs have shown significant advantages in controlling the water behavior, improving the dimensional and thermal stabilities [22–31]. The incorporation of inorganic materials into sulfonated polymers by cross-linking reaction has also been reported [32–39].

Polyhedral oligomeric silsesquioxane (POSS), $(RSiO_{1.5})_n$, an intermediate between silica (SiO_2) and silicone (R_2SiO), is a prototypical organic/inorganic system composed of hydrophobic inorganic core and externally covered by organic substituents. Through judicious design of the functionalities of the organic substituents, it is possible to create monofunctional or octafunctional macromonomer that can be incorporated into either linear thermoplastics or thermosetting networks to form high performance hybrid materials [40–51]. POSS hybrid materials are potential candidates for use in PEM because their relatively hydrophobic core as compared with sulfonated materials and adjustable external functionalities are able to affect the water behavior, dimension stability, and thermal stability of sulfonated polymers but rarely have been investigated [52]. In this study, properties of cross-linked PEMs comprising functionalized POSS and sulfonated poly(ether ether ketone) (SPEEK) are presented and discussed.

2. Experimental part

2.1. Materials

Toluene, DMSO, 4,4′-diaminodiphenyl ether (ODA), and platinum divinyltetramethyldisiloxane complex [Pt(dvs)] were purchased from Aldrich Chemical Co. Allyl glycidyl ether (AGE) was purchased from Acros Chemical Co. VICTREX PEEK grade 450G extruded pellets were purchased from Victrex. $Q8M8^H$ was obtained from Hybrid Plastics Co. Toluene and DMSO were distilled from calcium hydride. AGE was purified through vacuum distillation from calcium hydride before use. $Q8M8^H$, Pt(dvs), and ODA were used as received.

* Corresponding author. Tel./fax: +886 3 5131512.
E-mail address: changfc@mail.nctu.edu.tw (F.-C. Chang).

0032-3861/$ – see front matter © 2009 Elsevier Ltd. All rights reserved.
doi:10.1016/j.polymer.2009.11.033

2.2. Synthesis of octakis(dimethylsilyloxypropylglycidyl ether)octasilsesquioxane (OG-POSS) macromer

The $Q8M8^H$ macromer (1.96 mmol) was placed in a dry 50-mL round-bottom flask equipped with a stirrer bar, then anhydrous toluene (30 mL), AGE (16.66 mmol), and Pt(dvs) (0.2 mmol) were added. The reaction mixture was heated at 80 °C under an argon atmosphere for 8 h, then cooled to room temperature. The activated charcoal was added to the reaction mixture and stirred for 10 min, and the solution was filtered through a 0.45 mm Teflon membrane. The residual solvent was evaporated. The product, OG-POSS (Scheme 1), was obtained as a colorless and viscous liquid [42].

2.3. Synthesis of 4,4′-diaminodiphenyl ether-2,2′-disulfonic acid (ODADS)

ODA (8.00 g, 10.0 mmol) was placed under an argon atmosphere into a 100-mL three-neck flask equipped with a mechanical stirring device and cooled in an ice bath. Conc. H_2SO_4 (95%, 6.8 mL) was added for 10 min. After the ODA had been dissolved completely, fuming sulfuric acid (60% SO_3, 14 mL) was added dropwise to the flask. The sulfonation mixture was stirred at 25 °C for 2 h and then heated at 80 °C for an additional 4 h. The slurry was cooled to room temperature and then it was carefully poured onto crushed ice (100 g). The filtered white product was re-dissolved in a NaOH solution (30%, 500 mL), and then it was acidified with conc. HCl. The precipitate was filtered, washed repeatedly with deionized water and methanol, and then dried to constant weight [10].

2.4. Sulfonation of PEEK

The PEEK pellets (20 g) were added slowly to conc. H_2SO_4 (95–98 wt%, 500 mL) in a three-neck flask at room temperature under an argon atmosphere. After dissolution, the solution was heated at 55 °C with vigorous stirring for 3 h and then added to ice water to obtain the precipitate (SPEEK). After filtering and washing with distilled water, the SPEEK was converted into its sodium salt through immersion in 1 M NaOH for 72 h. The degree of sulfonation (DS) of the SPEEK was determined to be 71.8% by ^{1}H NMR in DMSO-d_6.

2.5. Membranes preparations

Desired amounts of SPEEK, OG-POSS, and ODA or ODADS were dissolved in DMSO to obtain 15% polymer solutions and these solutions were stirred for 24 h at 25 °C. The solutions were cast onto Teflon dishes maintained at 60 °C for 48 h to remove most of the solvent, and then the membranes were dried under vacuum at

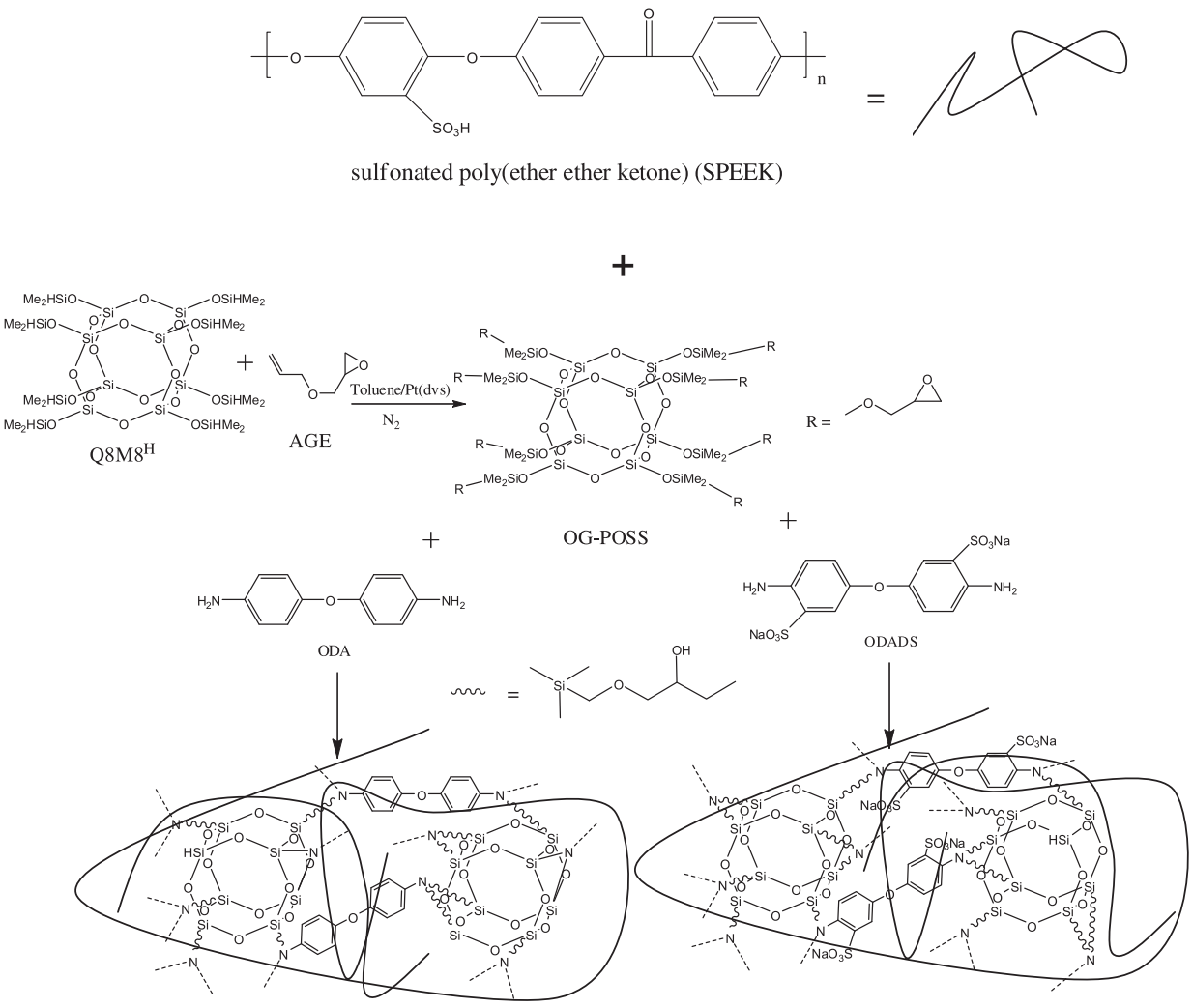

Scheme 1. Structure of the organic/inorganic networks.

about 0.2 torr at 60 °C for an additional 48 h to complete the drying process. Solid state ^{13}C NMR spectroscopy (Supporting Information, Fig. S1) demonstrated that the thermal curing reaction (Scheme 1) between OG-POSS and ODA (or ODADS) was complete during the first 48 h drying process. As shown in Fig. S1, the chemical shift at 69 ppm was attributed to the methylene carbon attached to amine (–CH_2–N) which formed from ring-opening reaction of the amine and epoxide groups. The chemical shifts at ca. 123, 132, and 149 ppm were corresponded to the aromatic carbons. Finally, the membrane was peeled off from the Teflon dish through immersion in deionized water. After immersion in 2 M HCl for 24 h, the film was obtained in acidic form, washed with deionized water until the pH reached 6–7. Table 1 summaries the membrane compositions.

2.6. Characterizations

^{13}C NMR spectrum was recorded at 25 °C on an INOVA 500 MHz spectrometer. The thermal degradation behavior of the membrane was measured using a thermal gravimetric analyzer (TGA Q100, TA) operated at a heating rate of 20 °C/min from 25 to 800 °C. Dynamic mechanical testing was performed using a DuPont DMA Q800 dynamic mechanical analyzer operated at a heating rate of 5 °C/min from 150 to 350 °C and a frequency of 1.0 Hz. Transmission electron microscopy (TEM) was performed using a JEOL JEM-1200CX-II microscope operated at 120 kV. To stain the hydrophilic domains, the membrane was converted into its Pb^{2+} form through immersion in 1 N $Pb(OAc)_2$ solution overnight and then rinsed with water. For TEM observation, the ultra-microtome section of the dried membrane (50-nm slices) was placed on 200-mesh copper grids.

2.7. Water uptake

The water uptake (WU; %) was calculated using Eq. (1):

$$\mathrm{WU}\ (\%) = \frac{W_{\mathrm{wet}} - W_{\mathrm{dry}}}{W_{\mathrm{dry}}} \times 100\% \tag{1}$$

where W_{wet} and W_{dry} are the wet weight and dried weight of the membrane, respectively. The completely dried PEM was immersed in deionized water at room temperature for 24 h, then removed quickly and blotted with filter paper to remove any excess water on the membrane surface, and immediately weighed to obtain its wet mass (W_{wet}). The dried weight (W_{dry}) of the membrane was measured after drying at 120 °C for 24 h [31].

2.8. Ion exchange capacity

The ion exchange capacity (IEC) was determined through titration with NaOH solution of the acid released from immersing the membrane with acid form into 1 M NaCl [31].

Table 1
Compositions of cross-linked proton exchange membranes.

	SPEEK (g)	OG-POSS (g)	ODA (g)	Cross-linker content (wt%)
OG03	2	0.06	0.0124	3.5
OG07	2	0.14	0.0290	7.8
OG10	2	0.2	0.0414	10.8
OG15	2	0.3	0.0621	15.3
OG20	2	0.4	0.0829	19.4
			ODADS (g)	
SOG03	2	0.06	0.0249	4.1
SOG07	2	0.14	0.0580	9.0
SOG10	2	0.2	0.0829	12.4
SOG15	2	0.3	0.1243	17.5
SOG20	2	0.4	0.1657	22.0

2.9. Bound water ratio

The amount of free water in the fully hydrated membranes was determined using a DuPont TA2010 differential scanning calorimeter. The sample was firstly cooled from 25 to −60 °C and then heated to 50 °C at a rate of 5 °C/min. The mass of free water in the membrane was measured by integrating the area under the cooling curve and comparing it to the enthalpy of fusion for water (314 J/g) [31].

2.10. Methanol diffusion coefficient

The methanol diffusion coefficient of the membrane was measured using a two-chamber liquid permeability cell that has been described in detail previously. A 50-mL chamber contained 5 M methanol solution; the other 50-mL chamber was filled with deionized water and continuous stirring. The methanol concentration in the water cell was determined periodically using a GC-8A gas chromatograph (SHTMADU, Tokyo, Japan). The methanol permeability was calculated using Eq. (2):

$$C_{\mathrm{B}}(t) = \frac{A}{V_{\mathrm{B}}}\frac{P}{L}C_{\mathrm{A}}(t - t_0) \tag{2}$$

where V_0 is the initial volume of deionized water, L is the membrane thickness, A is the membrane area, C_{A} and C_{B} are the methanol concentrations in the methanol and water chambers, respectively, and P is the methanol diffusion coefficient [31].

2.11. Proton conductivity

The frequency-dependent impedance property (from 10 kHz to 10 Hz) of these membranes was measured using an Autolab designed by Eco Chemie. For conductivity measurement, the membrane was placed in a conductivity cell between stainless-steel blocking electrodes at 30 °C and relative humidity (RH) of 100%. The conductivity was calculated according to Eq. (3)

$$\sigma = \frac{L}{AR_{\mathrm{b}}} \tag{3}$$

where σ is the conductivity, L is the membrane thickness, A is the section area of the stainless steel electrode, and R_{b} is the bulk resistance.

3. Results and discussion

3.1. Morphologies of cross-linkers

The degree of dispersion of POSS moieties in polymer matrices has great effect on both thermal and mechanical properties of resultant composite systems [40–51]. In this study, these OG-POSS/ODA and OG-POSS/ODADS cross-linkers were incorporated into PEMs. Membrane properties such as the water uptake, IEC, proton conductivity, and methanol permeability are expected to be affected because of the hydrophobic core and cubic structure of POSS. Previous reports on the morphologies of PEMs [1–39] and polymers containing various functionalized POSS derivatives [40–52] have indicated that the microstructure plays a critical role in determining their properties. Fig. 1 presents SEM images (cross-sectional views) of OG15 and SOG15 membranes. In Fig. 1(a), these OG-POSS/ODA cross-linkers (bright part) aggregate into various sized spherical domains (1–5 μm) in the OG15 membrane whereas these aggregated OG-POSS/ODADS domains are significantly smaller (100–300 nm) and better dispersed within the SOG15 membrane [Fig. 1(b)]. In the OG membrane, the OG-POSS/ODA cross-linkers

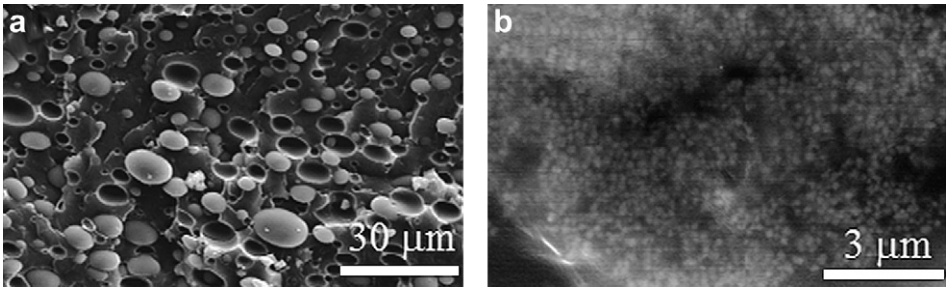

Fig. 1. SEM micrographs (cross-sectional views) of the (a) OG15 and (b) SOG15 membranes.

tend to aggregate into larger hydrophobic domains while these sulfonic acid groups of ODADS in the SOG membrane interact with both C═O and sulfonic acid groups of SPEEK and thus prevent excess aggregation of the OG-POSS/ODADS cross-linkers [53–56]. Therefore, large aggregation of the OG-POSS/ODA cross-linker occurs in the OG membrane system while the OG-POSS/ODADS cross-linkers aggregate into fine and well-distributed domains.

3.2. Thermal analyses

Fig. 2 presents the TGA curves of (a) SPEEK, OG03, and OG10 membranes and (b) OG03 and SOG03 membranes, indicating that all curves exhibit two steps of weight loss. The first degradation step above 300 °C corresponds to the degradation of sulfonic acid groups and the second weight loss region above 500 °C is associated with the degradation of the SPEEK main chain and linkages between the OG-POSS and ODA (or ODADS) units as previously reported [37,57]. These TGA curves suggest that all the membranes are suitable for use as proton conducting materials in terms of thermal stability. Fig. 2(b) reveals that the thermal stability of SOG03 membranes is slightly better than that of OG03 membranes. In addition, plots of loss factor tan δ as a function of temperature for SOG15 and OG15 membranes presented in Fig. 2(c) indicate that the glass transition temperature of the former is higher than that of the latter. In previous studies [53–56] the sulfonic acid group can interact with C═O group within the PEMs. In this study, the presence of sulfonic acid groups improves the miscibility between SPEEK and the OG-POSS/ODADS cross-linker and results in better distribution of cross-linkers and better thermal properties of these SOG membranes [58].

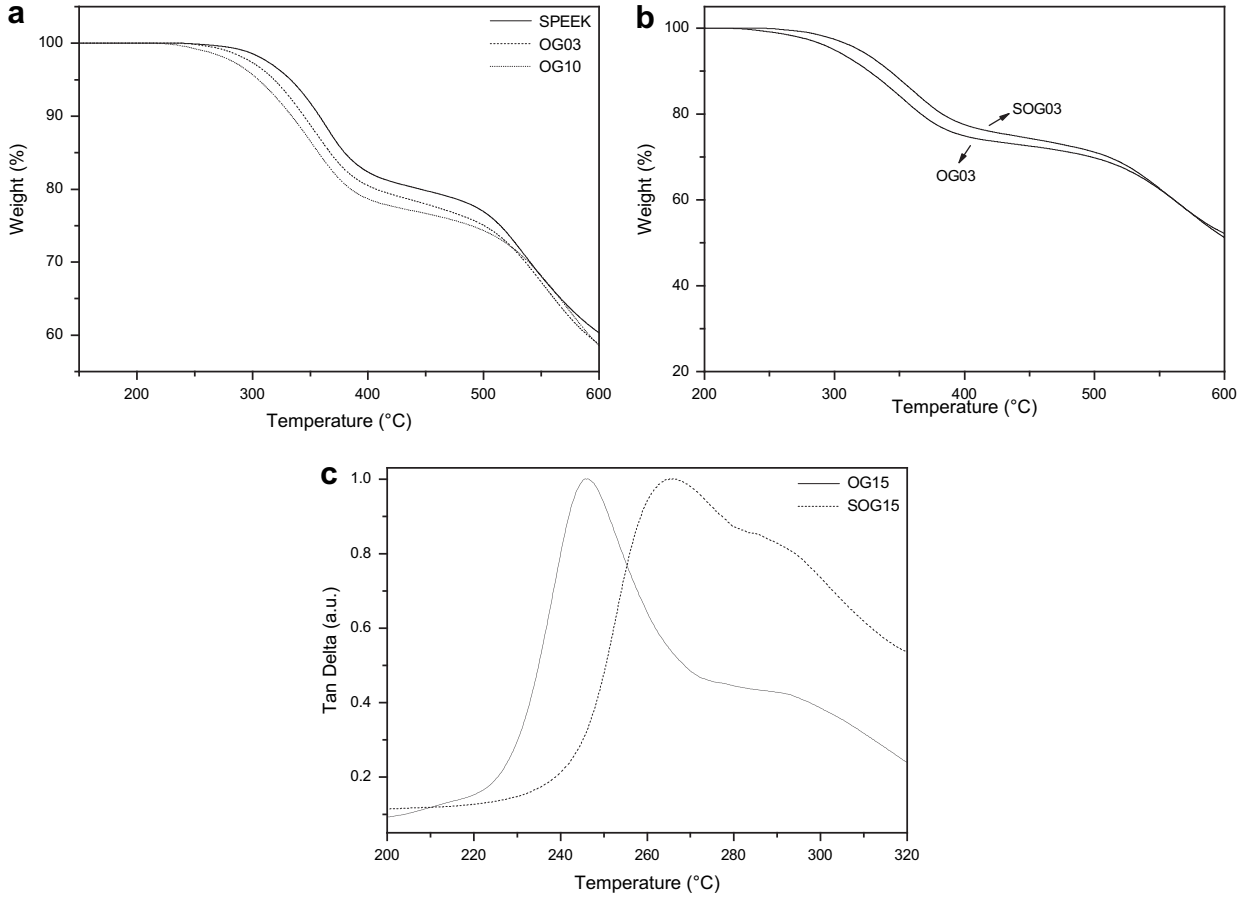

Fig. 2. TGA curves of the (a) SPEEK, OG03, and OG10 membranes and the (b) OG03 and SOG03 membranes. (c) Loss factors (tan δ) of OG15 and SOG15 (The corresponding storage modulus was listed in supporting information.).

3.3. Membrane morphologies

Fig. 3 displays TEM micrographs of the OG10 and SOG10 membranes where the light regions correspond to hydrophobic domains and these dark regions represent hydrophilic domains (ionic clusters). In Fig. 3(a), the size of the hydrophilic domains of SPEEK varies from very fine particles up to 100 nm, indicating that the SPEEK membrane hydrophilic domains are poorly distributed. The membranes measured by TEM measurement are all in anhydrous state; when they are fully hydrated, the hydrophilic domains tend to be connected to yield larger continuous hydrophilic domains and the resultant micro-phase separation of these hydrophilic/hydrophobic domains becomes more pronounced. Therefore, greater phase separation with continuous hydrophilic domains of the hydrated SPEEK membrane allows for easier proton transport through the Grotthus (hopping) and vehicle (diffusion) mechanisms. These features also affect the methanol permeability behavior because the methanol permeates through the formation of methanol/H_2O complexes (such as $CH_3OH_2^+$ and H_3O^+) through continuous hydrophilic domains. Fig. 3(b) reveals that the hydrophilic domains were separated and their size became more uniform in the OG10 membrane as compared with the SPEEK, essentially all these large hydrophilic domains are disappeared. The presence of OG-POSS/ODA cross-linkers tends to reduce the connectivity of hydrophilic domains. In Fig. 3(c), relative to OG10, the size of these hydrophilic domains within the SOG10 membrane is relatively smaller (20 nm) and better dispersed. The differences in the hydrophilic domain size and distribution between SOG10 and OG10 membranes can be attributed to the presence of the sulfonic acid groups of ODADS. Better distribution of the cross-linker units in the SOG10 membrane results in better separation of hydrophilic domains as compared with the OG10 and SPEEK membranes. When the OG10 membrane is hydrated, the connectivity of hydrophilic domains is relatively poorer than the SOG10 membrane because its hydrophilic domains are not distributed as well as the SOG10 membrane, resulting in lower methanol crossover and lower proton conductivity. Based on the above, as compared with these OG and SPEEK membranes, the SOG membrane is expected to exhibit high proton conductivity because the better distributed cross-linker units would result in adequate connectivity and dispersion of hydrophilic domains which are also able to decrease methanol crossover.

3.4. Relationship between water sorption and membrane miscibility

The extent of water molecules in PEMs affects the rate of proton transfer and methanol permeability. Excess water sorption causes reduced mechanical strength and poor hydrolytic stability of the PEM and thus unsuitable for fuel cell applications, implying the importance of water sorption. Fig. 4(a) indicates that the ion exchange capacity (IEC) depends on the content of sulfonic acid group in all these PEMs. When the OG-POSS/ODA cross-linker content is increased in the OG membranes, IEC decreases because of lower overall sulfonic acid content. In the SOG membranes, IEC increases with increasing cross-linker content due to the presence of the sulfonic acid groups in ODADS [24,59]. Fig. 4(b) displays the effect of the cross-linker content on the water uptake of OG and SOG membranes. All OG membranes exhibit lower water uptake relative to SPEEK and SOG membranes because of lower overall content of sulfonic acid groups and greater separation of hydrophilic domains [32–39]. On the other hand, the water uptakes of SOG03 and SOG07 membranes are higher than SPEEK and corresponding OG membranes, indicating that the relatively better distributed OG-POSS/ODADS cross-linker enhances the water sorption ability [24,59]. In the SOG10, SOG15, and SOG20 membranes, the water uptake decreases with increasing the cross-linker content because of the epoxy network structure which resulted in restriction on the SPEEK matrix.

Table 2 indicates that the bound water ratio affects the proton conductivity and methanol permeability of these PEMs. The bound water ratios of the OG membranes are all higher than that of the SPEEK membrane and increase upon increasing the cross-linker content as previous studies [24,59]. In contrast, the SOG03 membrane possesses the lowest bound water ratio as a result of the excess water sorption caused by the relative better distributed OG-POSS/ODADS cross-linkers. However, the bound water ratio

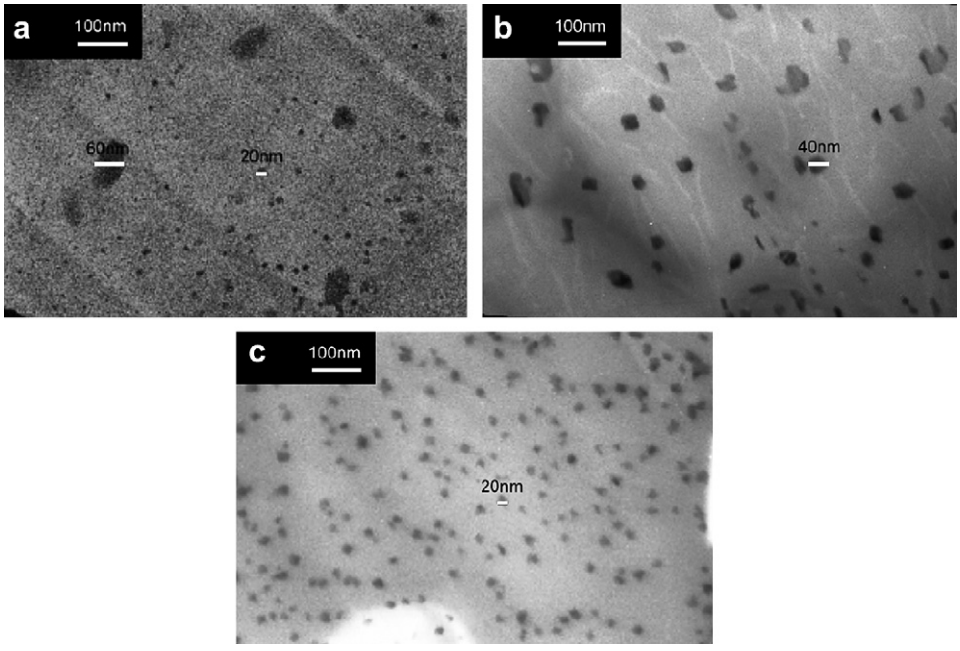

Fig. 3. TEM micrographs of the (a) SPEEK, (b) OG10, and (c) SOG10 membranes.

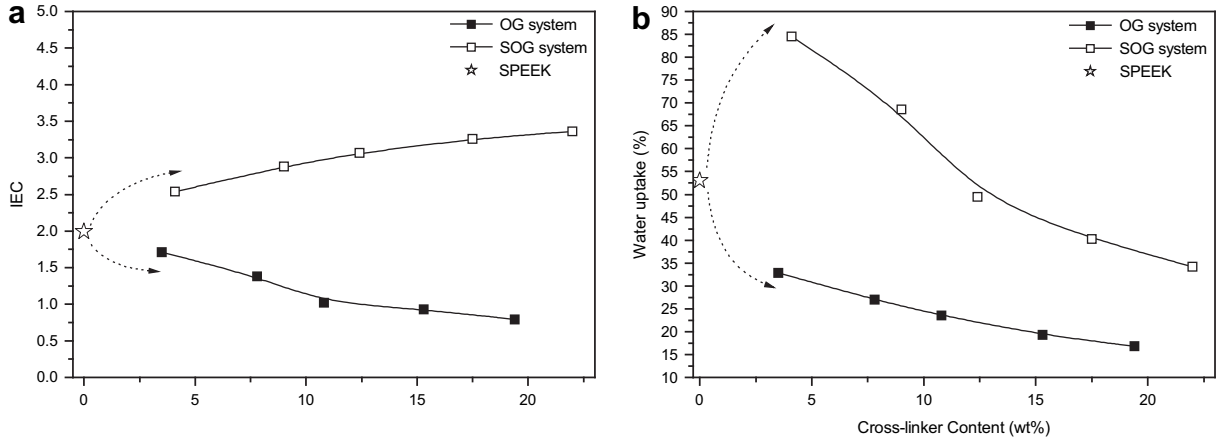

Fig. 4. (a) IEC values and (b) water uptakes plotted with respect to the cross-linker content for the SPEEK, OG, and SOG membranes.

increases upon further addition of OG-POSS/ODADS cross-linkers because the epoxy network structure resulting in restriction on the SPEEK matrix would dominate over the properties of the SOG membranes as previously described [24]. The water behavior of OG and SOG membranes are dependent upon the nature of cross-linkers and the characteristic of OG-POSS.

3.5. Proton conductivity, methanol permeability, and selectivity

Fig. 5(a) presents the proton conductivity as a function of the cross-linker content for OG and SOG membranes. All OG membranes exhibit lower proton conductivity than SPEEK and the proton conductivity decreases upon increasing the cross-linker content. The increase of the cross-linker content induces lower water uptake and thus lower proton conductivity. These proton conductivities of SOG03, SOG07, and SOG10 membranes are close or even higher than the SPEEK membrane, which is resulted from the relatively higher water uptake and better connected hydrophilic domain. In the SOG15 and SOG20 membranes, the effect of the epoxy network structure predominates over both morphology and the water behavior and thus results in lower proton conductivity.

Methanol permeability [Fig. 5(b)] is closely related to proton conductivity because methanol molecules are transported through the hydrophilic channels which also function as the proton transport medium. As mentioned above, the presence of OG-POSS/ODA cross-linkers in OG membranes dictates the distribution of hydrophilic domains and leads to the lower water uptake, lower free water content, and greater separation of hydrophilic domains. Therefore, all OG membranes exhibit lower methanol permeability than the SPEEK membrane. For SOG membranes, methanol permeabilities of SOG03 and SOG07 membranes are slightly higher or equal to the SPEEK membrane because of excess water uptake and lower bound water ratio. For SOG10, SOG15, and SOG20 membranes, the methanol permeability decreases upon increasing the cross-linker content because of the increased bound water ratio. Fig. 5(c) shows the selectivity of the OG and SOG membranes calculated from the ratio of proton conductivity to methanol permeability which can be used to judge whether they are suitable for PEM applications [25,33]. All OG membranes exhibit selectivities lower than the SPEEK membrane where methanol permeability and proton conductivity are both reduced after the incorporation of OG-POSS/ODA as a result of the relative higher degree of separation of hydrophilic domains, lower water sorption, and higher bound water ratio. Since the reduction in the proton conductivity dominates over the reduction in the methanol permeability, the resultant selectivities (performances) of all OG membranes are lower than the SPEEK membrane. On the other hand, all SOG membranes exhibit higher selectivities than the SPEEK membrane. Although both SOG03 and SOG07 possess higher methanol permeability as compared with pure SPEEK and OG membranes, they possess higher proton conductivities and thus higher selectivities. For SOG10, SOG15, and SOG20 membranes, their methanol permeabilities decrease while proton conductivities remain nearly unchanged with increasing the cross-linker content, thus their selectivites are higher than SOG03 and SOG07 membranes. The proton conductivities of SOG membranes remain

Table 2
Properties of cross-linked proton exchange membranes.

	Water uptake (%)	IEC (mequiv/g)	bound water ratio [bound]/[total]	Methanol permeability (cm^2/s)	Proton conductivity[a] (S/cm)	Selectivity (Ss/cm^3)
SPEEK	53.0	1.99	46.1	1.96×10^{-7}	0.0152 (152 μm)[b]	7.76×10^4
OG03	32.9	1.71	49.1	1.33×10^{-7}	0.0077 (143 μm)	5.78×10^4
OG07	27.0	1.38	55.6	1.02×10^{-7}	0.0055 (156 μm)	5.39×10^4
OG10	23.5	1.02	60.8	8.8×10^{-8}	0.0036 (138 μm)	4.09×10^4
OG15	19.3	0.93	67.8	6.3×10^{-8}	0.0028 (142 μm)	4.44×10^4
OG20	16.8	0.79	73.6	3.7×10^{-8}	0.0015 (146 μm)	4.05×10^4
SOG03	84.5	2.54	35.2	2.03×10^{-7}	0.0182 (135 μm)	8.96×10^4
SOG07	68.6	2.88	45.3	1.95×10^{-7}	0.0177 (144 μm)	9.07×10^4
SOG10	49.5	3.07	57.4	1.67×10^{-7}	0.0171 (139 μm)	1.02×10^5
SOG15	40.3	3.26	68.2	1.34×10^{-7}	0.0153 (129 μm)	1.14×10^5
SOG20	34.2	3.36	74.5	1.08×10^{-7}	0.0119 (135 μm)	1.10×10^5

[a] The proton conductivity was measured at 30 °C and RH of 100%.
[b] The thickness of the membrane used for the proton conductivity measurement.

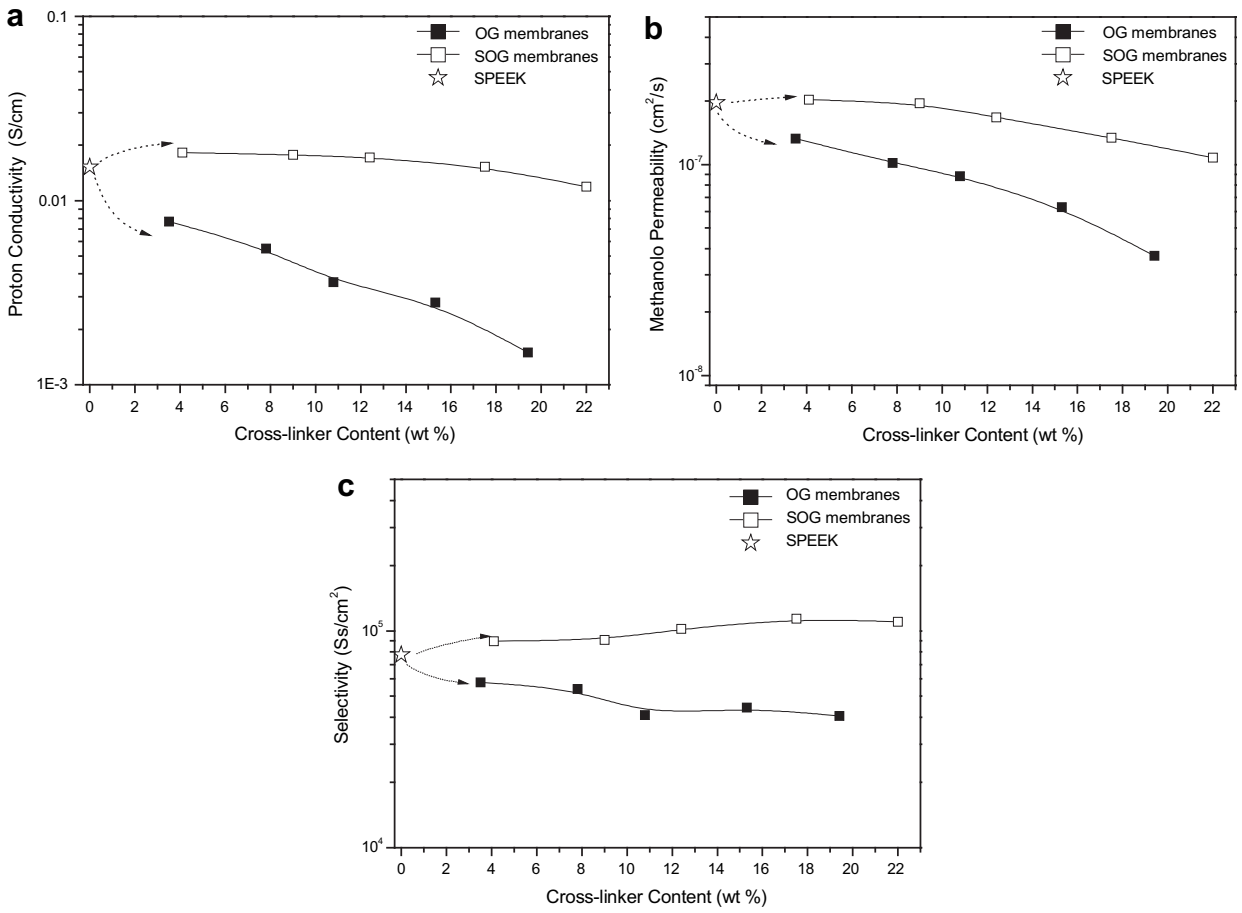

Fig. 5. (a) Proton conductivities, (b) methanol permeabilities, and (c) selectivities plotted with respect to cross-linker content for SPEEK, OG, and SOG membranes.

nearly unchanged due to relatively better distribution of these OG-POSS/ODADS cross-linkers which results in complex connection of separated hydrophilic domains as observed in SEM and TEM micrographs. Fig. 6 illustrates the proposed mechanisms of proton transfer within these PEMs. In the OG system, the OG-POSS/ODA crosslinkers tend to aggregate into relatively hydrophobic domain, resulting in separated hydrophilic domains. The protons tend to be conducted through Grotthus mechanism. Thus, the OG membranes possessed relatively lower proton conductivity and methanol permeability. However, the presence of sulfonic acid groups attached to ODADS in the SOG system is able to interact with both carbonyl and sulfonic acid groups of SPEEK which can prevent the aggregation of OG-POSS molecules, resulting in smaller and better distributed OG-POSS/ODADS domains than in the OG system. The protons within SOG membranes were transported through both Grotthus and vehicle mechanisms and the SOG membranes possess better and complex connection of hydrophilic domains that tend to hinder methanol crossover without significant affecting the proton conductivity. Therefore, SOG membranes exhibit higher proton conductivities, lower methanol permeabilities, and higher selectivities as compared with those OG and SPEEK membranes.

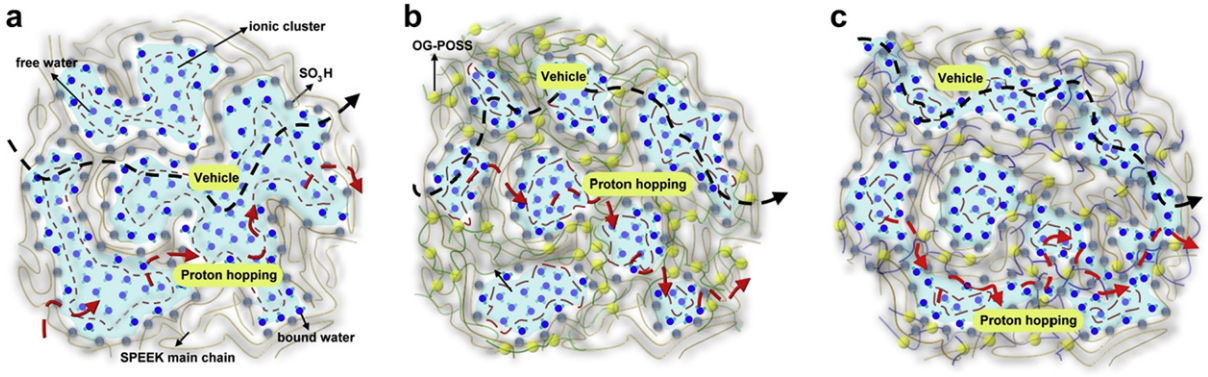

Fig. 6. Proposed mechanisms of proton transfer within the (a) SPEEK (b) OG, and (c) SOG membranes.

4. Conclusions

A new cross-linked proton exchange membrane comprising SPEEK and an epoxy network containing OG-POSS nanoparticles was prepared. From a comparison of the properties between the OG and SOG membranes, the latter are substantially better than the former in terms of selectivity because of better distribution of the sulfonic acid containing OG-POSS/ODADS cross-linkers. In addition, better distribution of the OG-POSS/ODADS cross-linker causes higher bound water ratio and better complex connection of hydrophilic domains within these SOG membranes. The typical SOG membrane, SOG15, possesses relatively higher proton conductivity (0.0153 S/cm), lower methanol permeability (1.34×10^{-7} cm^2/s), and higher selectivity (1.14×10^5 Ss/cm^3).

Supplementary data

Supplementary data associated with this article can be found, in the online version, at doi:10.1016/j.polymer.2009.11.033.

References

[1] Hickner MA, Ghassemi H, Kim YS, Einsla BR, McGrath JE. Chem Rev 2004;104:4587.
[2] Bai Z, Houtz MD, Mirau PA, Dang TD. Polymer 2007;48:6598.
[3] Rozière J, Jones DJ. Ann Rev Mater Res 2003;33:503.
[4] Xing PX, Robertson GP, Guiver MD, Mikhailenko SD, Kaliaguine S. Macromolecules 2004;37:7960.
[5] Wang Z, Ni HZ, Zhao CJ, Li XF, Zhang G, Shao K, et al. J Membr Sci 2006;285:239.
[6] Schönberger F, Jochen Kerres JJ. Polym Sci Pol Chem 2007;45:5237.
[7] Patric Jannasch P. Curr Opin Colloid Interface Sci 2003;8:96.
[8] Fu YZ, Manthiram A, Guiver MD. Eelctrochem Commun 2007;9:905.
[9] Xing PX, Robertson GP, Guiver MD, Mikhailenko SD, Wang KP, Kaliaguine SJ. J Membr Sci 2004;229:95.
[10] Fang JH, Guo XX, Harada S, Watari T, Tanaka K, Kita H, et al. Macromolecules 2002;35:9022.
[11] Zhou ZL, Dominey RN, Rolland JP, Maynor BW, Pandya AA, DeSimone JM. J Am Chem Soc 2006;128:12963.
[12] Miyatake K, Chikashige Y, Eiji Higuchi E, Watanabe M. J Am Chem Soc 2007;129:3879.
[13] Asano N, Aoki M, Suzuki S, Miyatake K, Uchida H, Watanabe MJ. Am Chem Soc 2006;128:1762.
[14] Xu K, Li K, Khanchaitit P, Wang Q. Chem Mater 2007;19:5937.
[15] Zhang C, Hirt DE. Polymer 2007;48:6748.
[16] Subbaraman R, Ghassemi H, Zawodzinski TA. J Am Chem Soc 2007;128:2238.
[17] Yamaguchi T, Zhou H, Nakazawa S, Hara N. Adv Mater 2007;19:592.
[18] Grunzinger SJ, Watanabe M, Fukagawa K, Kikuchi R, Tominaga Y, Hayakawa T, et al. Power Sources 2008;175:120.
[19] Li Y, VanHouten RA, Brink AE, McGrath JE. Polymer 2008;49:3014.
[20] Shi ZQ, Holdcroft S. Macromolecules 2005;38:4193.
[21] Farhat TR, Hammond PT. Adv Funct Mater 2005;15:945.
[22] Ding FC, Wang SJ, Xiao M, Meng YZJ. Power Sources 2007;164:488.
[23] Cho KY, Jung HY, Shin SS, Choi NS, Sung SJ, Park JK, et al. Electrochim Acta 2004;50:589.
[24] Lee CH, Park HB, Chung YS, Lee YM, Freeman BD. Macromolecules 2006;39:755.
[25] Fu TZ, Zhao CJ, Zhong SL, Zhang G, Shao K, Zhang HQ, et al. Power Sources 2007;165:708.
[26] Qiao JL, Hamaya T, Okada T. Chem Mater 2005;17:2413.
[27] Zhong SL, Fu TZ, Dou ZY, Zhao CJ, Na HJ. Power Sources 2006;162:51.
[28] Gasa JV, Boob S, Weiss RA, Shaw MT. J Membr Sci 2006;269:177.
[29] Yamaki T, Kobayashi K, Asano M, Kubota H, Yoshida M. Polymer 2004;45:6569.
[30] Park HB, Lee CH, Sohn JY, Lee YM, Freeman BD, Kim HJ. J Membr Sci 2006;285:432.
[31] Ye YS, Yen YC, Cheng CC, Chen WY, Tsai LT, Chang FC. Polymer 2009;50:3196.
[32] Kim DS, Liu BJ, Guiver MD. Polymer 2006;47:7871.
[33] Chen WF, Kuo PL. Macromolecules 2007;40:1987.
[34] Shahi VK. Solid State Ionics 2007;177:3395.
[35] Vona MLD, Marani DD, Ottavi C, Trombetta M, Traversa E, Beurroies I, et al. Chem Mater 2006;18:69.
[36] Kim DS, Park HB, Rhim JW, Lee YM. J Membr Sci 2004;240:37.
[37] Su YH, Liu YL, Sun YM, Lai JY, Wang DM, Gao Y, et al. J Membr Sci 2007;296:21.
[38] Chen SW, Holmberg B, Li WZ, Wang X, Deng WQ, Munoz R, et al. Chem Mater 2006;18:5669.
[39] Chang YW, Wang E, Shin G, Han JE, Mather PT. Polym Adv Technol 2007;18:535.
[40] Ragosta G, Musto P, Abbate M, Scarinzi G. Reactivity, viscoelastic behaviour and mechanical performances of hybrid systems based on epoxy resins and reactive polyhedral oligosilsesquioxanes. Polymer 2009;50:5518–32.
[41] Huang KW, Tasi LW, Kuo SW. Polymer 2009;50:4876.
[42] Randriamahefa S, Lorthioir C, Guégan P, Penelle J. Polymer 2009;50:3887.
[43] Goldman M, Shen L. Phys Rev 1966;114:321.
[44] Tamaki R, Choi J, Laine RM. Chem Mater 2003;15:793.
[45] Mijovic J, Bian Y. Polymer 2009;50:1541.
[46] Wu J, Haddad TS, Mather PT. Macromolecules 2009;42:1142.
[47] do Carmo DR, Paim LL, Dias NL. Appl Surf Sci 2007;253:3683.
[48] Yen YC, Ye YS, Cheng CC, Chen HM, Sheu HS, Chang FC. Polymer 2008;49:3625.
[49] Yen YC, Kuo SW, Huang CF, Chen JK, Chang FC. J Phys Chem B 2008;112:10821.
[50] Misra R, Alidedeoglu AH, Jarrett WL, Morgan SE. Polymer 2009;50:2906.
[51] Lichtenhan JD. In: Salamone JC, editor. Polymeric materials encyclopedia. Boca Raton, FL: CRC Press; 1996. p. 7768.
[52] Chang YW, Wang E, Shin G, Han JE, Mather PT. Polym Adv Technol 2007;18:535.
[53] Devrim YG, Rzaev Z, Piskin E. Macromol Chem Phys 2007;208:175.
[54] Robertson GP, Mikhailenko SD, Wang KP, Xing PX, Guiver MD, Kaliaguine SJ. J Membr Sci 2003;219:113.
[55] Zhang HB, Pang JH, Wang D, Li AZ, Li XF, Jiang ZH. J Membr Sci 2005;264:56.
[56] Gao Y, Robertson GP, Guiver MD, Jian X, Mikhailenko SD, Wang K, et al. Polym Sci Part A: Polym Chem 2003;41:2731.
[57] Yu JF, Ngo T, McLean G. Chem Mater 2005;17:387.
[58] Liu HZ, Zheng S, Nie KM. Macromolecules 2005;38:5088.
[59] Lin CW, Huang YF, Kannan AM. J Power Sources 2007;164:449.